Progress In Electromagnetics Research, Vol. 112, 155–181, 2011

RAINFALL RATE PROBABILITY DENSITY EVALUATION AND MAPPING FOR THE ESTIMATION OF RAIN ATTENUATION IN SOUTH AFRICA AND SURROUNDING ISLANDS

P. A. Owolawi

Department of Electrical Engineering
Mangosuthu University of Technology
Umlazi, KwaZulu-Natal, South Africa

Abstract—The paper describes the modelling of the average rainfall rate distribution measured at different locations in South Africa. There are three major aspects this paper addresses: to develop a rainfall rate model based on the maximum likelihood method (ML); to develop contour maps based on rainfall rate at 0.01% percentage of exceedence; and re-classification of the ITU-R and Crane rain zones for the Southern Africa region. The work presented is based on five-minute rainfall data converted to one-minute equivalent using a newly proposed hybrid method. The results are mapped and compared with conventional models such as the ITU-R model, Rice-Holmberg, Moupfouma and Crane models. The proposed rainfall rate models are compared and evaluated using root mean square and chi-square (χ^2) statistics. Then re-classification of the rain zone using ITU-R and Crane designations is suggested for easy integration with existing radio planning tools. The rainfall rate contour maps at 0.01% percentage of exceedence are then developed for South Africa and its surrounding islands.

1. INTRODUCTION

Signal transmission at microwave and millimeter bands provides several advantages over lower frequency bands which include extensive bandwidth, frequency re-use, small antenna as well as short time deployment. The propagation of waves in this frequency range is predominantly by line-of-sight propagation and thus, there are certain

Received 25 August 2010, Accepted 26 November 2010, Scheduled 11 January 2011
Corresponding author: Pius Adewale Owolawi (owolani@mut.ac.za).

phenomena which affect the signal strength at these bands. The most important factor to take into consideration at these bands is the attenuation and scattering due to rain [1]. The simplest approach to employ in estimating rain attenuation is to use measured rainfall rate statistics where applicable. If this is not available, modeled rainfall rate statistics for a specified geographic region should be considered [2].

In fact, a lot of research has been conducted in the area of rainfall rate modeling, and expressions to determine rainfall rate value at given percentages of exceedence has been proposed. The most widely known models are Crane's Global Climatic Model [3], the ITU-R P-837 recommendation [4], originally developed under CCIR in 1974 and now in its fifth revision under ITU-R. Other rainfall rate distribution models commonly referred to by many workers in this field are Rice-Holmberg's model [5], Moupfouma et al. model [6], and Ajayi and Ofoche model [7]. In the Southern Africa, similar research has been conducted by Owolawi et al., Fashuyi et al., and Mulangu et al. [8–14]. The work done and reported by Seeber [15] for South Africa and the surrounding islands of Marion and Gough was based on 15-minute integration time. This approach is not very suitable for system planners because the high integration time used may not respond to rapid changes in the cumulative distribution of rainfall rate.

The works done in [11, 12] are based on rainfall rate integration time conversion factors of a location in South Africa and as stated in the papers, the results were generalized for other stations. In the recent work submitted [16], a hybrid method was proposed for the conversion of rain rate from 5-minute integration time to 1-minute equivalent; which involves regional parameters that influence the rainfall rate distribution curves.

1.1. Review of Existing Rain Rate Models

Rain rate modelling is an important component used in the estimation of rain attenuation and thus, the fade margins for a specified geographical region. The models are often classified into two classes which are: global and localized rain rate models.

In global rain rate models, the mechanism used primarily depends on climatic parameters and geographical locations. There are several global rain rate models available but for the purpose of this paper, the two models considered are two are Crane's and ITU-R global models.

The work done by Crane [3] classified the globe into eight regions; each labelled **A** through **H** with varying degrees of dryness to wetness. The ITU-R provides another global rain rate climatic model termed characteristics of precipitation for propagation modelling. The model was originally developed under CCIR in 1974 and several revisions have been made from ITU-R P837-1 to recently revised ITU-R P.837-5 [4].

Although both Crane and ITU-R global climatic models are widely known and adopted by many telecommunication companies to plan their link budget, they may not be adequate to account for seasonal and yearly variation. This dynamic variation of rainfall is not uncommon in South Africa's climatic zones as confirmed by other researchers in their localities. In the comparison carried out with the previous ITU-R recommendations [17], South America's tropical zone was confirmed to have a large area, the Crane's global model classified it as zone **H**, thus it has 209.7 mm/hr rain rate at 0.01% percentage of exceedence [3]; while the ITU-R recognised the zone as three different rain zones of 80 mm/hr, 100 mm/hr and 120 mm/hr. This means that the difference between the rain rates estimated by the two models is about 100%.

In many sites in South Africa and surrounding Islands, a similar trend of large variation is observed. In Durban, the ITU-R P.837-1 mapped rain rate to be 22 mm/hr at 0.01%, the ITU-R P.837-5 suggested 50 mm/hr while Crane represented the rain rate by 46.8 mm/hr. The trend of variation between P.837-1 to P.837-5 is about 39% difference. The percentage difference between P.837-1 and Crane's suggested rain rate is 36%. In the enforce ITU-R P.837-5 the difference between ITU-R and Crane is 3.3% for Durban. This latter result shows a better improvement in the ITU-R global climatic rain rate model. In summary, the prime advantage of global rain rate is that even in the absence of lofty spatial resolution of point rain rate information, estimation of rain rate can be determined at a given percentage of exceedence using universal climatic information to characterize each of the regions of the globe. The limitations of the previous ITU-R recommendations such as discontinuity is taken care off in the enforce recommendation but the effects of cyclic year, variability and seasonal changes are still issues to be rectified.

In the case of local rain rate models, researchers from different parts of the world have proposed several regional based rainfall rate models. These rain rate models are developed from empirical equations using results of field measurements collected over a long period of years. Rain rate climatic models in this category which deserves to be mentioned include Rice-Holmberg model [5], Dutton-Dougherty-Martin model [20], Crane two-component model [3], Moupfouma-Martin model [6], and Seeber rain rate model [15].

2. EXPERIMENTAL MEASUREMENT FACILITIES

The rainfall data employed in this study has been collected by two different rain measuring equipment. Measurements have been obtained by means of Oregon Rain gauge and Joss-Waldvogel Distrometer (JWD). In addition, over ten years rainfall data with five-minute integration time has been provided by the South Africa Weather Service (SAWS).

An Oregon rain gauge (RGR 382) was installed at the Latitude (30°58'E) and Longitude (29°52'S) with an altitude of 139.7 meters at the School of Electrical, Electronics and Computer Engineering in the University of KwaZulu-Natal, Howard College campus. The rain gauge collector has a diameter measuring 101.6 mm, and stands 146.05 mm high. The gauge contains a collecting bucket that tips after accumulation of 1 mm of rainfall. The measuring accuracy of the bucket with rain rate of 0–15 mm per hour is $+/-10\%$ while above 15 mm per hour is $+/-15\%$. The gauge functioned for a period of one-year (2005–2006).

The Joss-Waldvogel distrometer is an instrument for measuring raindrop size distribution (DSD). This equipment is not limited to measuring raindrop distribution only, but is also incorporated into precipitation field measurement purposely to validate and complement the measurements of the rain gauge. The distrometer used in this study is capable of measuring rain rate, reflectivity, rain accumulation, raindrop size (diameter range 0.3–5.5 mm) at 60-second intervals with an accuracy of 5%. For the current study, the distrometer was installed in December 2008, and commenced operation in January 2009 with a sampling interval integrated over one minute. Both the rain gauge and Joss-Waldvogel distrometer are present at the master site (control site) and located approximately 2 meters from each other. The site is free of noise and shielded from abnormal winds.

Finally, the South Africa Weather Services (SAWS) provides rainfall data of five-minute integration time for over ten years for all the provinces in South Africa and the surrounding Islands. SAWS use different means to collect their precipitation data. The most widely used method is via a network of rain gauges. Rain gauges used by SAWS are standard 127 mm in accordance with the World Meteorological Organization (WMO) standard. The 127 mm is the diameter of the rimmed circular funnel opening. The other type of rain gauge used by SAWS is the automated rain gauge, which is a tipping bucket rain gauge with a 200 mm funnel opening. The data used in this study is based on the specification and calibration of the two types of rain gauges mentioned. In the case of distrometer, 92%

of its data was processed and used while less than 2.8% of the data provided by South Africa Weather Services was not used.

3. 1-MINUTE INTEGRATION TIME: HYBRID METHOD

In the initial attempt to model rain rate distribution for South Africa as explained in Fashuyi et al. [10], a conversion factor constants was used to convert hourly rainfall data to its one-minute equivalent. The conversion factor which was originally based on the available one-minute and hourly data was used to propose the model. However, one-minute rain rate data is neither sampled at the same time nor in the same place as the hourly rain rate data.

In the hybrid method as detailed in [16] combined optimized proposed 1-minute rain rate conversion model based on one available 1-minute regional rain rate. Polynomial model is considered for conversion of rain rate from five-minute to one-minute equivalent for South Africa and surrounding Islands with a general expression given as:

$$R_1(p_i) = aR_5(p_i)^2 + bR_5(p) + c \tag{1}$$

where a, b and c are constants. In the case of Durban, it is noted that $a = 0.0014$, $b = 1.2021$ and $c = -0.3543$. The other expressions used in equiprobable method are the power fit and linear fit given as:

$$R_1(p_i) = d\,[R_5(p_i)]^e \tag{2}$$

$$R_1(p_i) = f\,[R_5(p_i)] + g \tag{3}$$

where d, e, f and g are constants with values for Durban given by 1.063, 1.046, 1.334 and −2.115, respectively. The hybrid approach is adopted to estimate one-minute rain rate for other provinces in South Africa and the surrounding islands, and mapped using Koppen climatic classification method. The Koppen and coefficients for conversion factors are given in Figure 4 and Table 6 of [16] respectively.

3.1. Improvements on the New Proposed Rain Rate Model

In the initial attempt to model rain rate distribution for South Africa, a general conversion factor was used. Fashuyi et al. [10] and Owolawi and Afullo [11] employed the power law expression to convert available 60-minute rain rate to a one-minute equivalent for the twelve South African sites. This modelling theory was based on the approach employed by Moupfouma and Martin [6] in which the relative values were determined for eight sites in South Africa. However, these current studies improve on the limitations of that initial proposed rain rate model which may not be adequate in describing the rain rate due to the following reasons:

- Lack of one-minute rain rate to carry out conversion processes using power laws for the entire country and surrounding islands;
- Unavailability of long term rain data to develop the model that takes care of cyclic years;
- Fitting of the rain rate data with other established rain rate models may lead to the concession of the model parameters.

In this new proposed approach, all these factors are taken into consideration and are properly and adequately addressed. The current proposal uses a maximum likelihood estimator to fit different statistical distributions. The work presented is based on more than ten years five-minute rainfall data converted to a one-minute equivalent using a newly developed hybrid model.

In addition to the ten years rainfall data, the other parameters employed in this work are average annual total rainfall M (mm/yr), the highest monthly precipitation M_m (mm/month), the average number of thunderstorm day in a year (Dth) day which are extracted from World Meteorological organization documents 1953 and 1962 [18, 19] and estimated ratio of convective rain or thunderstorm to the total average rainfall accumulation (β) as expressed in Dutton et al. [20].

3.2. Performance of the Proposed Conversion Method

As explained in [16], there are two levels of test carried on the proposed hybrid model. The first level of test is employed to confirm which of the three sets of hybrid model distribution is suitable for the region by using relative error method with their average standard deviation (STD) and average root mean square (RMS). The test is carried out at the control site (Durban) where actual 1-minute and 5-minute rainfall data are available. Table 1 shows the best fit distribution that describes the proposed one-minute rain rate (Hybrid method) with measured one-minute rain rate. The average value of the absolute relative error is noted to be lowest when the polynomial fit of second order is used, while the maximum average error is observed with power law fit. The same trend is observed for the cases when STD and RMS of relative errors are used.

At 0.01% percentage of exceedence, the power fit seems to be the best with a 9.88% relative error, whereas the linear and polynomial fits give 14.79% and 12.28% of relative error, respectively. This is confirmed by the RMS value where the power fit records a value of 0.97%, while polynomial and linear fits record 1.5% and 2.1%,

Table 1. Comparison between the different fit distributions for Durban using average, STD, and RMS values.

First level test	**Average value of absolute** $E_{\mathrm{Rel},i}(\%)$	**STD value of absolute** $E_{\mathrm{Rel},i}(\%)$	**RMS value of absolute** $E_{\mathrm{Rel},i}(\%)$
Linear Fit	11.72	12.38	16.69
Polynomial fit (2nd order)	6.74	6.21	9.0
Power Fit	14.64	5.0	15.40
ITU-R P.837-5	10.85	7.05	12.80
New Proposed ITU-R	9.0	4.78	10.72

respectively. At 0.001% percentage of exceedence, the performance of the polynomial fit is the best with a 0.072% of relative error, while the error for the linear fit is 1.68%, with highest relative error observed in power fit. Comparisons between ITU-R P.837-5 and the proposed new global power model using Durban's data shows that the percentage difference between the existing ITU-R and proposed ITU-R's global model in this study are 9.31%, 19.18%, and 8.85%, when using average value of absolute error, standard deviation of absolute value of error, and root mean square of absolute error, respectively. The performance of the polynomial fit of second order is considered the best for conversion of rain rate from five-minute to the one-minute equivalent because the average error evaluation confirms the polynomial fit as the overall best performing regression fit compared to its other counterparts.

In the second evaluation, absolute percentage relative error, RMS and APR (average probability ratio) are used to optimize and compare the propose hybrid method against the existing models and the measured rain rate data. The Chi-square statistic is used to confirm the acceptance or rejection of the null hypothesis of the compared models. A good model should give an APR close to 1, a minimum *absolute* $\varepsilon(p)$ and minimum RMS. It should also give a χ^2 statistic that is lower than the threshold t_δ for a defined probability value δ for $N-1$ degree of freedom (DF). In this work, δ is chosen to be 5%.

In Table 2, the result of the evaluation defined over the interval of 1% to 0.001% is presented. From the table, the absolute relative error records its least value of 3.08% in the case of Hybrid model (Polynomial type) and highest in the case of Rice-Holmberg model with 63.22%. The other models that fall below 10% of absolute relative errors are Hybrid (Linear type), ITU-R P.837-5, Australia model,

Table 2. Comparison between the measured data, proposed models and existing.

Second level test	Absolute % Relative Error	RMS	APR	CHI 5%/12.592
Segal model (Singapore)	9.00	8.67	1.00	5.27
Burgueno modes (Singapore)	9.64	7.99	0.99	4.89
Rice-Holmberg model (Dutton et al.)	63.22	47.15	2.94	171.31
Ito et al. (Japan)	19.28	15.69	1.25	17.02
Lavergnat et al. model	9.58	3.70	1.06	1.76
Ajayi et al. model (West Africa)	10.79	5.51	1.01	3.66
USA (Texa)	34.32	30.45	1.55	65.54
Canada (Montreal)	37.25	34.68	1.67	85.40
Italy (Rome)	23.33	21.63	1.31	32.03
Australia (Flavin)	7.16	3.73	1.04	1.40
China (Xiao et al.)	11.19	3.40	1.08	1.80
ITU-R P.837-5	6.59	8.09	1.02	4.45
Brazil model (Maritime Tropical)	9.62	4.95	0.91	3.32
Brazil model (Equatorial)	10.16	3.87	1.02	1.82
New propose ITU-R	14.08	10.31	1.18	7.50
Hybrid (Polynomial Law)	3.08	2.97	0.98	1.07

Hybrid (Power type), fitted Segal (Singapore) model, Lavergnat et al. model and Brazil model (Maritime tropical) in descending order error values. The reason for the lower relative error recorded may be due to similarity in the geographical patterns of the region especially in the case of Australia. Considering RMS and APR error for the same mentioned models, it seems that similar trends are observed. Using the χ^2 evaluation at 5% confidence interval, it is observed that some models could be used to convert from five-minute rain rate integration time to its one-minute equivalent. As inferred from Table 2, the proposed Hybrid model with polynomial fit performs better than the others.

4. PROBABILITY THEORY OF THE PROPOSED RAIN RATE MODEL

Since it may be impossible to provide rainfall data for the prediction of attenuation due to rain at any instant in future, a probabilistic model is then required for system designer for both terrestrial and satellite link designs. In this section, three distribution models with their maximum likelihood estimators are presented. The preferred distributions are Weibull, Lognormal and Gamma, which are widely used to describe precipitation distribution pattern over a defined period. They are described as follow:

I. Two parameters Weibull distribution: the probability density of 1-minute rain rate at a give probability of exceedence $R_1(p)$ mm/hr is given as [21]:

$$f(R_1(p))=\left\{\begin{matrix} \frac{\alpha}{\beta}\left(\frac{R_1}{\beta}\right)^{\alpha-1}\exp\left[-\left(\frac{R_1}{\beta}\right)^{\alpha}\right], & R_1(p)\geq,\alpha\triangleright,\beta\triangleright 0 \\ 0 & \text{elsewhere}\end{matrix}\right\} \quad (4)$$

and the distribution is given as:

$$F(R_1(p))=\left\{\begin{matrix} 1-\exp\left[-\left(\frac{R_1}{\beta}\right)^{\alpha}\right], & R_1(p)\geq,\alpha\triangleright,\beta\triangleright 0 \\ 0 & \text{elsewhere}\end{matrix}\right\} \quad (5)$$

where $\alpha\triangleright 0$ is the shape parameter and $\beta\triangleright 0$ is the scale parameter. Suppose that rain rate $R_1(p)$ is observation at different percentage of exceedence which is denoted by $p_1, p_2, p_3, \ldots p_N$. The likelihood function may be given as

$$\ln L = N\ln\alpha - N\alpha\ln\beta + (\alpha-1)\sum_{i=1}^{N}\ln R(p_i) - \sum_{i=1}^{N}\left(\frac{R(p_i)}{\beta}\right)^{\alpha} \quad (6)$$

The maximum likelihood estimate of parameters $\hat{\alpha}$ and $\hat{\beta}$ assumed solution at condition when:

$$\frac{\partial \ln L}{\partial \alpha} = 0 \quad (7)$$

$$\frac{\partial \ln L}{\partial \beta} = 0 \quad (8)$$

N denotes sample size and the Newton-Raphson approximation method is used to solve simultaneous equations at the rth iterative by the expression:

$$\begin{aligned}\hat{\alpha}(r) &= \alpha(r-1) + h(r)\\ \hat{\beta}(r) &= \beta(r-1) + k(r)\end{aligned} \quad (9)$$

where $h(r)$ and $k(r)$ are the correction terms given in the Equation (10) [21, 22]:

$$\begin{bmatrix} h \\ k \end{bmatrix} = \begin{bmatrix} \frac{\partial^2 \ln L}{\partial \alpha^2} & \frac{\partial^2 \ln L}{\partial \alpha \partial \beta} \\ \frac{\partial^2 \ln L}{\partial \beta \partial \alpha} & \frac{\partial^2 \ln L}{\partial \beta^2} \end{bmatrix}^{-1} \begin{bmatrix} -\frac{\partial \ln L}{\partial \alpha} \\ -\frac{\partial \ln L}{\partial \beta} \end{bmatrix} \tag{10}$$

In this work, the iteration is terminated at the point of convergence where the correction terms lies below approximately 0.002. The derivation to all first order and second order derivatives are presented in the Appendix A of [21].

II. Two parameters lognormal distribution: the lognormal with two parameters, μ and σ represent location and scale parameters, respectively. The probability density of 1-minute rain rate at a given probability of exceedence $R_1(p)$ mm/hr as expressed by Evans et al. [23] and Walack [24] as:

$$f(R_1(p)) = \frac{\exp\left(-\frac{1}{2}\left(\frac{\ln R_1(p)-\mu}{\sigma}\right)^2\right)}{x\sigma\sqrt{2\pi}} \quad 0 \leq R_1(p) < +\infty \tag{11}$$

where σ = scale parameter of the included normal distribution ($\sigma > 0$), μ = location parameter of the included normal distribution.

Here, the maximum likelihood estimation for the two-parameter lognormal used is given by Eckhard et al. [25] and Suhaila and Jemain [26] as:

$$\hat{\mu} = \exp\left(\frac{1}{n}\sum_{i=1}^{N}\log R(p_i)\right) = \left(\prod_{i=1}^{N} R(p_i)\right)^{\frac{1}{N}} \tag{12}$$

$$\hat{\sigma} = \exp\left|\left(\frac{1}{N-1}\sum_{i=1}^{N}\left[\log\left(\frac{R(p_i)}{\hat{\mu}}\right)\right]^2\right)^{\frac{1}{2}}\right| \tag{13}$$

The mean (μ) of rain rate data $R_1(p)$ and the standard deviation (σ) are calculated. The $\hat{\mu}$ and $\hat{\sigma}$ are then estimated using the expressions $\mu/\sqrt{\omega}$ and $\exp(\sqrt{\log(\omega)}$, respectively, with $\omega = 1 + (\sigma/\mu)^2 = 1 + CV^2$. [Note CV is called coefficient of variation with the expression given as $CV = (\exp(\sigma^2) - 1)^{0.5}$].

III. Two parameters Gamma distribution: two parameters gamma distribution probability density function for rain rate $R_1(p)$ is given as [23]:

$$f(R_1(p)) = \frac{1}{\beta^\gamma \Gamma(\gamma)} R_1(p)^{\gamma-1}\exp(-R_1(p)/\beta), \quad \gamma, \beta \triangleright 0, R_1(p) \triangleright 0 \tag{14}$$

where γ and β are the shape and scale parameters, respectively and Γ is denote gamma function. Considering a given data set of rain rate $R_1(p)$, maximum likelihood estimates of γ and β can be estimated by solving the following equations by Thom [27], the approximate expression to estimate $\hat{\gamma}$ is given as:

$$\hat{\gamma} = \frac{1 + (1 + 4A/3)^{0.5}}{4A} \tag{15}$$

$$\hat{\beta} = N\hat{\gamma} / \sum_{i=1}^{N} R_1(p_i) \tag{16}$$

where $A = \log \bar{x} - (\sum_{i=1}^{N} \log R_1(p_i))/N$.

4.1. Application of the Model

The proposed model in Section 4 is applied on rain rate data for all the provinces in South Africa and the surrounding Islands. Figure 1 shows sample histograms of one-minute integration time of rainfall rate estimated from its equivalent five-minute rainfall data for a period of ten years using methods and equations described in Section 4. The probability density functions plots of each distribution are superimposed on each histogram as shown in Figure 1. This

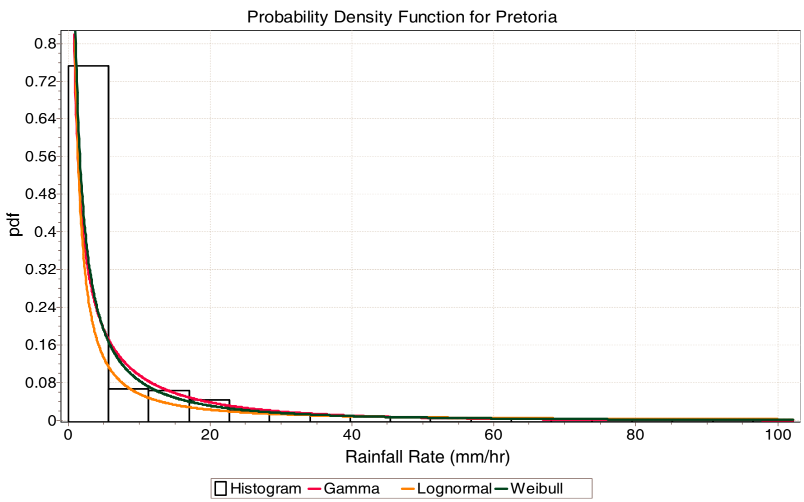

Figure 1. Sample histogram with Gamma, Lognormal and Weibull probability density function for Pretoria.

method is considered for twenty-one stations in South Africa and two surrounding Islands. Estimates for six parameters given as $(\hat{\alpha}, \hat{\beta}, \hat{\sigma}, \hat{\mu}, \hat{\gamma}, \hat{\beta})$ for Weibull, lognormal and gamma distributions are shown in Table 3.

The results displayed in Table 3 suggests possible variation in the distributions of rain rate both in terms of seasonal, periodical or cyclic effect in the climatological years. As may be seen from the table, the average values for Weibull parameters ($\hat{\alpha} = 0.43$ $\hat{\beta} = 3.13$), lognormal parameters ($\hat{\sigma} = 1.51$ $\hat{\mu} = 0.84$) and gamma parameters ($\hat{\gamma} = 0.16$ $\hat{\beta} = 53.64$). The dispersion of the distributions shows less than 1 in the three tested distributions except in the case of $\hat{\beta}$ in Weibull and gamma that record values that is greater than 1.

Table 3. Estimates of distribution parameters for the three distributions.

Location	W-B Parameters	L-G Parameters	G-M Parameters
Port-Alfred	$\hat{\alpha} = 0.31$ $\hat{\beta} = 1.26$	$\hat{\sigma} = 1.03, \hat{\mu} = 1.52$	$\hat{\alpha} = 0.18$ $\hat{\beta} = 39.87$
Bisho	$\hat{\alpha} = 0.31$ $\hat{\beta} = 1.40$	$\hat{\sigma} = 1.03, \hat{\mu} = 1.35$	$\hat{\alpha} = 0.16$ $\hat{\beta} = 53.64$
Fort Beaufort	$\hat{\alpha} = 0.38$ $\hat{\beta} = 1.77$	$\hat{\sigma} = 1.03$ $\hat{\mu} = 0.90$	$\hat{\alpha} = 0.14$ $\hat{\beta} = 41.58$
Umtata	$\hat{\alpha} = 0.32$ $\hat{\beta} = 1.90$	$\hat{\sigma} = 1.03$ $\hat{\mu} = 1.04$	$\hat{\alpha} = 0.24$ $\hat{\beta} = 39.87$
Pretoria	$\hat{\alpha} = 0.46$ $\hat{\beta} = 3.45$	$\hat{\sigma} = 2.18$ $\hat{\mu} = 0.06$	$\hat{\alpha} = 0.27$ $\hat{\beta} = 25.66$
Bethlehem	$\hat{\alpha} = 0.34$ $\hat{\beta} = 3.25$	$\hat{\sigma} = 2.63$ $\hat{\mu} = 0.56$	$\hat{\alpha} = 0.29$ $\hat{\beta} = 37.46$
Durban	$\hat{\alpha} = 0.71$ $\hat{\beta} = 9.40$	$\hat{\sigma} = 1.31$ $\hat{\mu} = 1.54$	$\hat{\alpha} = 0.34$ $\hat{\beta} = 35.56$
Spring	$\hat{\alpha} = 0.37$ $\hat{\beta} = 4.61$	$\hat{\sigma} = 2.15$ $\hat{\mu} = 0.03$	$\hat{\alpha} = 0.24$ $\hat{\beta} = 39.87$
Ladysmith	$\hat{\alpha} = 0.44$ $\hat{\beta} = 3.45$	$\hat{\sigma} = 1.83$ $\hat{\mu} = 0.08$	$\hat{\alpha} = 0.23$ $\hat{\beta} = 34.99$
Pietermaritzburg	$\hat{\alpha} = 0.41$ $\hat{\beta} = 2.88$	$\hat{\sigma} = 1.86$ $\hat{\mu} = 0.31$	$\hat{\alpha} = 0.19$ $\hat{\beta} = 41.70$
Tshipise	$\hat{\alpha} = 0.43$ $\hat{\beta} = 3.50$	$\hat{\sigma} = 1.94$ $\hat{\mu} = 0.12$	$\hat{\alpha} = 0.31$ $\hat{\beta} = 26.38$
Ermelo	$\hat{\alpha} = 0.42$ $\hat{\beta} = 3.20$	$\hat{\sigma} = 1.94$ $\hat{\mu} = 0.22$	$\hat{\alpha} = 0.23$ $\hat{\beta} = 36.40$
Cape Town	$\hat{\alpha} = 0.28$ $\hat{\beta} = 0.47$	$\hat{\sigma} = 0.94$ $\hat{\mu} = 1.62$	$\hat{\alpha} = 0.17$ $\hat{\beta} = 20.73$
Beaufort	$\hat{\alpha} = 0.67$ $\hat{\beta} = 6.28$	$\hat{\sigma} = 1.39$ $\hat{\mu} = 1.09$	$\hat{\alpha} = 0.32$ $\hat{\beta} = 26.80$
Cape Point	$\hat{\alpha} = 0.32$ $\hat{\beta} = 1.03$	$\hat{\sigma} = 1.06$ $\hat{\mu} = 1.58$	$\hat{\alpha} = 0.18$ $\hat{\beta} = 32.50$
Rustenburg	$\hat{\alpha} = 0.35$ $\hat{\beta} = 1.71$	$\hat{\sigma} = 1.5$ $\hat{\mu} = 0.27$	$\hat{\alpha} = 0.31$ $\hat{\beta} = 28.11$
Klerksdorp	$\hat{\alpha} = 0.79$ $\hat{\beta} = 5.27$	$\hat{\sigma} = 1.09$ $\hat{\mu} = 1.06$	$\hat{\alpha} = 0.31$ $\hat{\beta} = 19.85$
Kimberley	$\hat{\alpha} = 0.30$ $\hat{\beta} = 1.61$	$\hat{\sigma} = 1.08$ $\hat{\mu} = 1.48$	$\hat{\alpha} = 0.24$ $\hat{\beta} = 30.78$
Upinton	$\hat{\alpha} = 0.64$ $\hat{\beta} = 2.97$	$\hat{\sigma} = 1.28$ $\hat{\mu} = 0.38$	$\hat{\alpha} = 0.17$ $\hat{\beta} = 27.14$
Gough Island	$\hat{\alpha} = 0.35$ $\hat{\beta} = 2.55$	$\hat{\sigma} = 1.56$ $\hat{\mu} = 0.77$	$\hat{\alpha} = 0.33$ $\hat{\beta} = 24.20$
Marion Island	$\hat{\alpha} = 0.42$ $\hat{\beta} = 1.15$	$\hat{\sigma} = 1.31$ $\hat{\mu} = 1.08$	$\hat{\alpha} = 0.21$ $\hat{\beta} = 16.55$

4.2. Comparison and Goodness of Fit Test of the Distributions with Existing Models

In this section, the root mean square method is applied to test the goodness-of-fit and robustness of the proposed models (that are based on statistical distributions) with Weibull lognormal and Gamma rainfall distribution models. In addition, a Chi-square test is carried out on all twenty-three sites to confirm acceptance or rejection of the hypothesis in both the distributions and existing models. Figure 2 shows a comparison of the rainfall rate at equal percentage of exceedence for one of the selected stations. The percentage probability of exceedence chosen is based on the ITU-R specified range of 1% to 0.001%. Estimated rainfall rate is compared with distributions such as two-parameter Weibull (W-B), two-parameter lognormal (L-G), two-parameter Gamma (G-M). The estimated rainfall rate is also compared with existing models such as Rice-Holmberg (R-H), ITU-R P.837-1, P.837-5, Crane Global model (C-R), Moupfouma and Martin for tropical/sub-tropic (M-ST) and temperate (M-TE).

Figure 2 shows that the estimated rainfall rate distribution patterns are similar in shape when compared with the described distributions and existing models except in the case of Rice-Holmberg which distribution is almost linear in shape. The only sites that Rice-

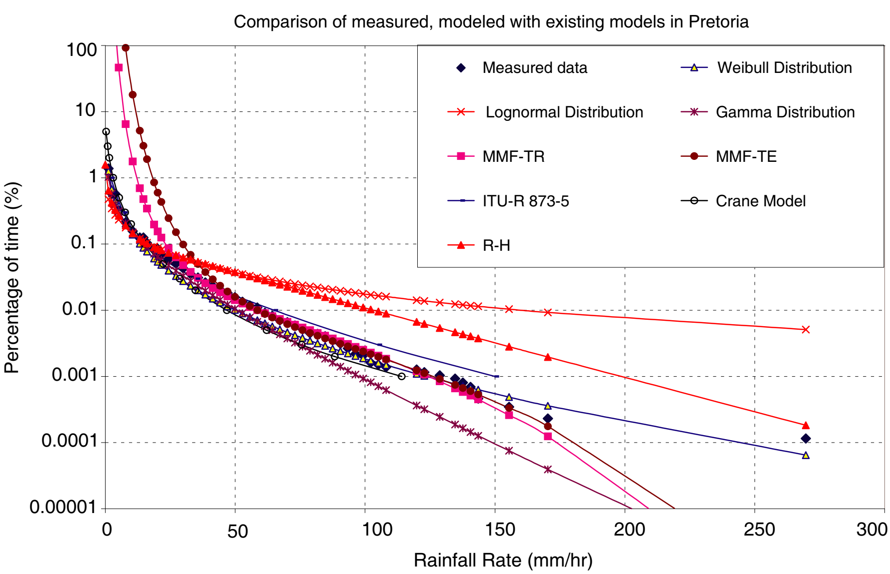

Figure 2. Comparison samples of estimated one-minute rainfall rate with the distributions and existing models in Pretoria.

Holmberg distribution describes properly are Gough Island, Marion Island, Upington and Klerksdop. ITU-R recommendations P.837-1 and P.837-2 give the same pattern distribution of estimated rainfall but does not properly fit into the data (especially that of ITU-R P.837-1). The ITU-R P.837-5, that is currently in-force, gives a better description of sites such as Pretoria, Ermelo, Cape Town, and the other two Islands. These mentioned locations may be sampled sites for ITU-R as well as Crane Global for extrapolation of rain climatic zones for South Africa and the surrounding Islands. In this work, both Weibull and Gamma distributions show a better description of the estimated rainfall rate distribution for the majority of the selected sites; the Crane distribution model shows reasonably acceptable distribution in some sites such as Pretoria and Cape Town.

Tables 4 and 5 show the statistical analysis carried out on twenty-one stations using the two statistical optimization methods. Table 4 shows the numeric results of root mean square (RMS). The average RMS values indicates that the Gamma model has the best performance with about 4.23% of the total RMS, while Rice-Holmberg model has the least performance with 19.36% of the total RMS. W-B, M-TE, and

Table 4. Comparison using root mean square error.

Location	W-B	L-G	G-M	R-H	ITU-R 1	ITU-R 5	C-R	M-ST	M-TE
Port-Alfred	8.366	16.273	11.239	17.04	53.83	44.00	38.78	11.43	6.13
Bisho	13.11	35.18	12.29	14.62	64.60	55.15	41.72	33.18	13.85
Fort Beaufort	14.54	42.48	13.09	15.89	34.71	40.38	37.23	20.07	10.57
Umtata	8.49	40.68	7.42	16.05	38.52	43.35	33.09	14.34	9.72
Pretoria	5.47	57.47	7.54	33.06	27.31	6.92	8.88	7.86	9.71
Bethlehem	29.80	92.62	8.60	45.80	61.49	15.11	46.99	11.69	32.77
Durban	22.34	64.50	10.14	85.26	54.28	34.85	29.30	11.31	24.04
Spring	19.33	81.49	11.76	88.98	15.96	40.64	16.22	16.22	13.81
Ladysmith	11.40	60.11	13.05	68.77	45.78	15.47	15.58	12.02	23.44
Pietermaritzburg	22.89	36.74	24.64	27.28	59.96	40.49	33.96	19.40	14.64
Tshipise	12.11	57.06	5.09	48.35	17.26	23.51	17.42	15.07	10.93
Ermelo	12.92	73.19	12.83	78.45	47.31	8.55	47.31	11.32	21.11
Cape Town	15.54	13.46	2.30	56.02	18.27	2.59	2.89	9.71	2.79
Beaufort	9.43	61.11	14.85	53.56	26.42	8.38	11.29	13.30	7.56
Cape Point	11.26	13.45	2.85	69.52	33.48	16.12	18.29	8.55	14.27
Rustenburg	11.93	48.67	2.58	50.63	32.50	16.89	20.09	7.44	14.05
Klerksdorp	17.32	6.15	5.14	20.01	18.38	28.87	6.20	15.06	7.71
Kimberley	22.84	5.0	4.83	73.59	32.13	16.72	19.82	17.33	9.60
Upinton	23.75	14.89	7.42	18.20	21.20	26.32	9.71	17.28	20.88
Gough Island	3.39	5.13	3.48	6.31	17.40	7.27	13.33	6.73	7.96
Marion Island	13.06	48.24	14.10	4.69	39.32	7.24	36.46	14.61	4.65

Table 5. Comparison using chi-square statistics.

Location	W-B	L-G	G-M	R-H	ITU-R 1	ITU-R 5	C-R	M-ST	M-TE
Port-Alfred	10.73	18.42	7.30	28.37	164.21	129.99	90.14	60.36	50.27
Bisho	9.91	55.43	7.32	34.39	196.27	150.85	97.88	106.99	66.52
Fort Beaufort	12.70	97.83	8.77	30.42	71.93	92.90	79.02	102.32	80.86
Umtata	8.76	94.75	3.67	23.62	95.85	108.76	68.10	87.81	72.66
Pretoria	4.19	260.07	4.84	90.85	73.86	4.44	8.47	42.26	41.63
Bethlehem	11.07	347.0	4.83	110.62	143.09	17.12	99.49	19.09	52.95
Durban	26.47	179.63	6.02	384.15	176.51	73.60	53.66	103.92	104.60
Spring	19.34	323.37	8.10	490.58	21.66	490.58	21.66	100.69	79.06
Ladysmith	11.76	167.60	11.47	269.70	139.98	16.73	17.29	86.90	105.06
Pietermaritzburg	34.08	228.08	32.33	223.70	189.78	82.93	56.85	86.61	73.93
Tshipise	18.34	249.72	12.54	157.16	30.15	65.89	112.34	194.32	174.22
Ermelo	14.72	263.47	11.85	352.73	148.09	5.72	148.09	105.30	194.27
Cape Town	19.51	42.00	1.37	470.88	34.86	2.06	1.57	13.84	6.17
Beaufort	51.99	350.97	68.69	214.34	59.45	7.97	12.20	53.85	41.46
Cape Point	9.57	16.94	1.13	548.42	89.90	27.20	31.14	27.60	35.51
Rustenburg	17.98	132.29	0.65	156.08	92.69	16.14	35.18	30.99	36.43
Klerksdorp	33.36	4.48	6.92	31.72	35.54	75.52	4.78	22.84	11.43
Kimberley	31.15	9.58	2.05	409.10	82.64	19.36	30.49	33.25	22.06
Upinton	44.94	18.46	5.24	8.27	55.62	38.15	76.61	9.86	24.05
Gough Island	2.31	3.42	1.80	14.72	40.09	7.60	25.57	34.53	49.00
Marion Island	23.98	191.89	20.11	4.14	157.78	10.98	138.59	25.09	3.18

M-ST have percentage values of less than 15% of the total RMS values. The ITU-R 1, ITU-R 5 and C-R have percentage values between 10% and 17% of total RMS values.

Table 5 shows the comparison of the performance of the models through the Chi-square results for 40 degrees of freedom, the threshold for 1% significance is 63.7. A small Chi-square value corresponds to a better fit of the distribution or model. Table 5 shows that the Gamma distribution gives the lowest χ^2 statistics for 76% of the stations (16 out of 21). For Pretoria, the best distribution is Weibull, followed closely by ITU-R P837-5 and Gamma. The exception is Beaufort site, where the Gamma distribution hypothesis is rejected; instead, the ITU-R P837-5 best represents the site, followed by the Crane model. The reasons may be due to mix climatic classification of mid-latitude desert and mid-latitude steppe characteristics. In addition, it has lowest monthly rain accumulation of approximate 35 mm/hr and annual rainfall accumulation of 236 mm/hr. In spite of the uniqueness of Beaufort, the Gamma model seems to be the best for the Southern African region, with an average χ^2 statistic of 10.8 over the 21 stations. The next distribution model that appropriately describes the rainfall rate distribution well in Southern Africa is the Weibull model, with an average χ^2 statistic of 19.85. The other models give average χ^2 statistics of above 55, which is rather too close to the threshold of 63.7. Although they fall under acceptable threshold of the Chi-square, they may be least considered to describe rainfall rate distributions for the Southern Africa.

5. RAINFALL RATE RE-ZONING FOR SOUTH AFRICA AND SURROUNDING ISLANDS

As rain rate becomes the principal component in determining rain attenuation when planning terrestrial and satellite links at higher frequency. It may be a time-consuming process to evaluate a large number of sites [17]. The use of ITU-R and Crane's designations may be of advantage over other models because many radio and satellite planning tools are designed around these two major types of designations. Since one of the applications of this paper is to provide information regarding rain rate distribution to system designers and radio design tools developers, it will be of advantage to adapt the regional re-zoning using the existing designations of ITU-R and Crane. Majority of researchers often conclude that ITU-R model either over-estimates or under-estimates the rainfall rate at a certain defined percentage of exceedence. Figures 3 and 4 compare the rainfall rate distributions with ITU-R rain climate zone designations while Figures 5 and 6 show the Crane's climatic rain zones for different sites in South Africa and its surrounding islands. Here the closest designation distribution to the measured data is chosen.

5.1. Comparative Studies of both ITU-R and Crane Rain Rate Zones

The reclassification is based on the chi-square optimization method. In Figure 3, Port Alfred shows that the currently enforced ITU-R P837-5 differs from the ITU-R P837-1 by 29.62%. The newly assigned designation of rain zone L with chi-square statistic of 7.16 at six degrees of freedom and at 5% confidence level differs from ITU-R P837-5 by 26.31%. Its counterpart, the Crane rain zone, as shown in Figure 5 considered D_2 as the appropriate zone for the region and differs from the old designation of C by 22.67%. For the same degrees of freedom, the chi-square test confirmed Crane's D_1 and ITU-R L rain climatic zones for Bisho with 13.65% and 9.09% differences from the old designations respectively. Pietermaritzburg and most of the studied sites showed that ITU-R and Crane's rain climatic zone under-estimate rainfall rate at 0.01% except in the case of Tshipise and Kimberley

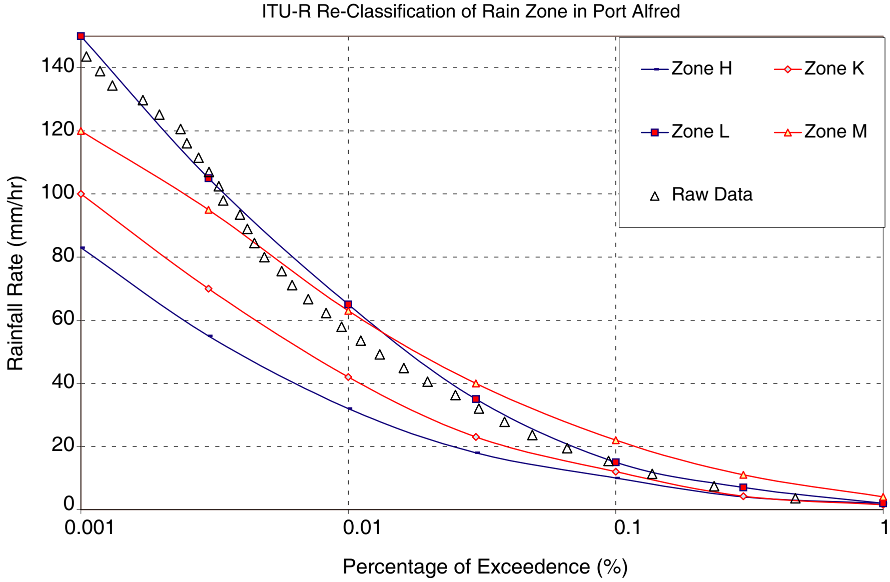

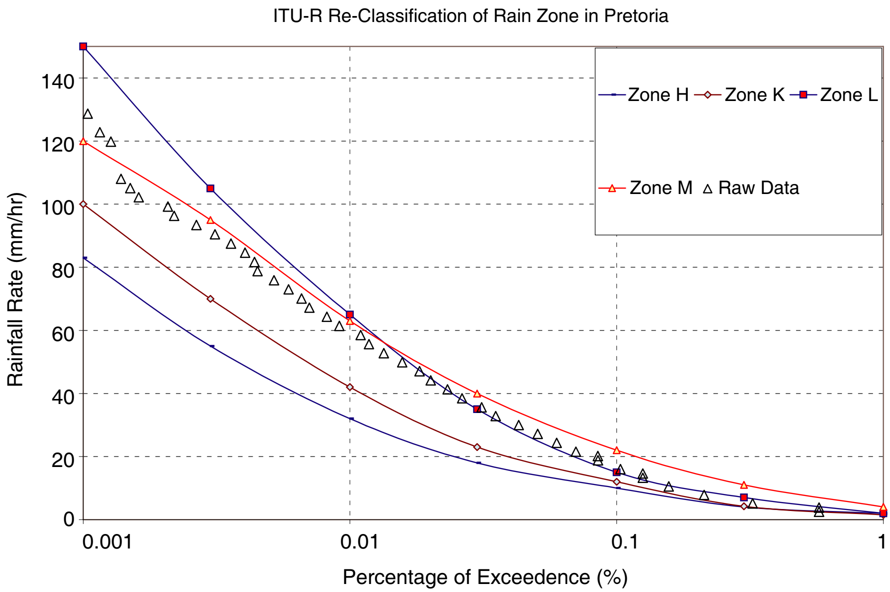

Figure 3. ITU-R rain classification re-zoning for South Africa and surrounding islands.

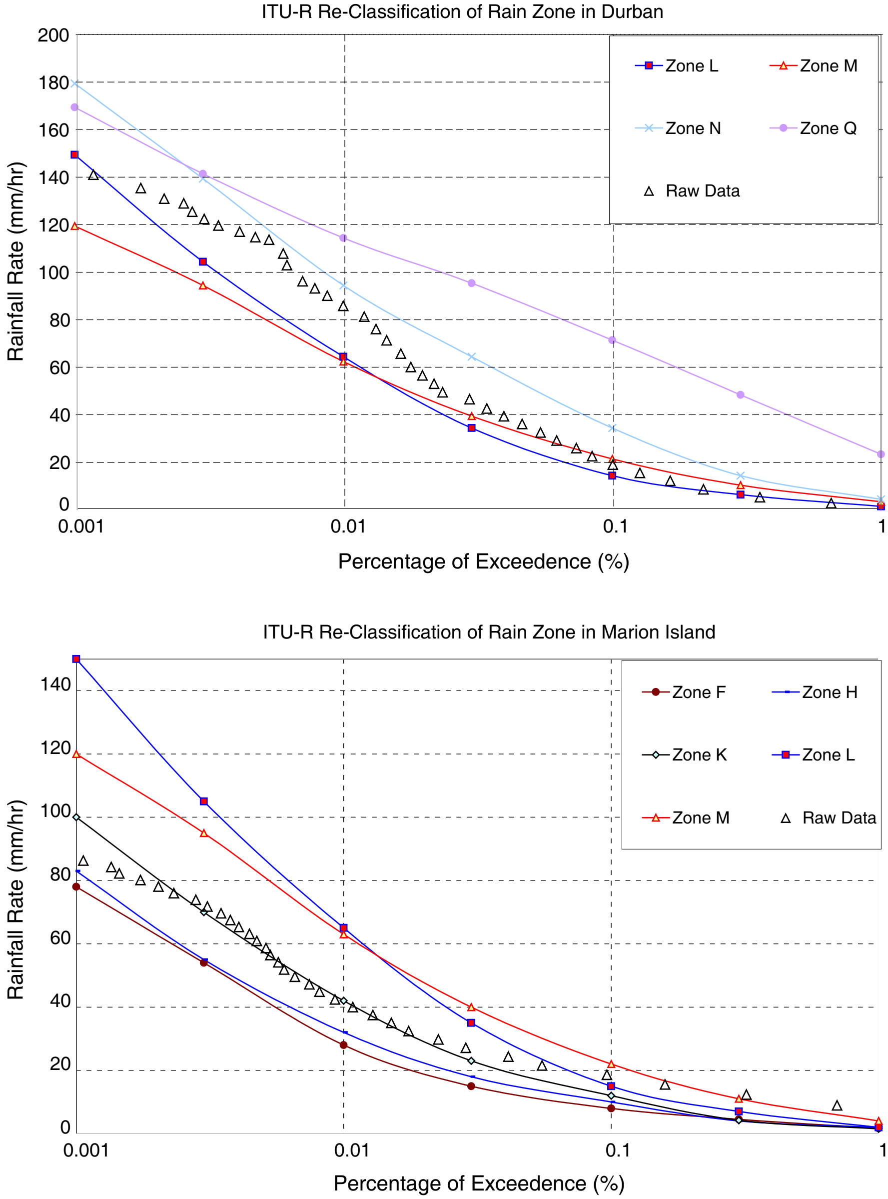

Figure 4. ITU-R rain classification re-zoning for South Africa and surrounding islands.

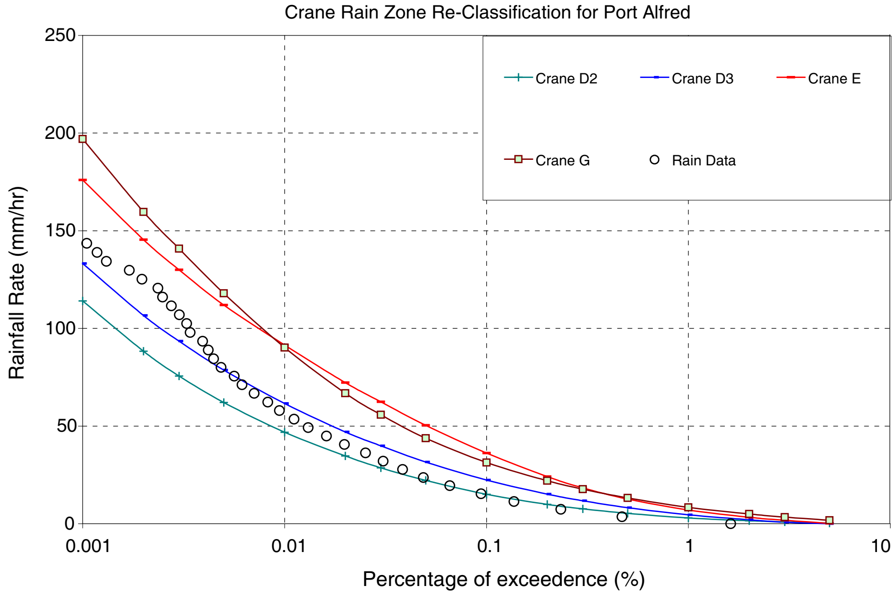

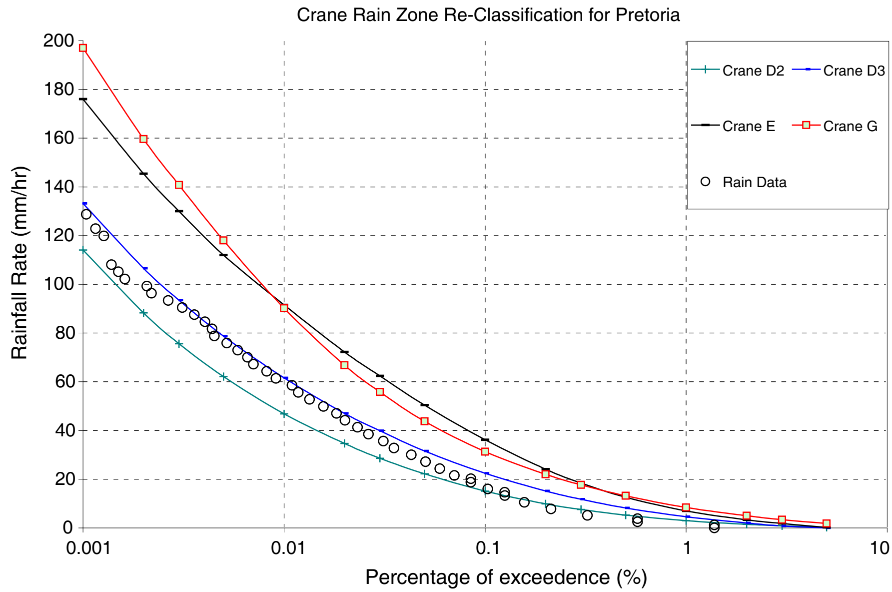

Figure 5. Crane rain classification re-zoning for South Africa and surrounding islands.

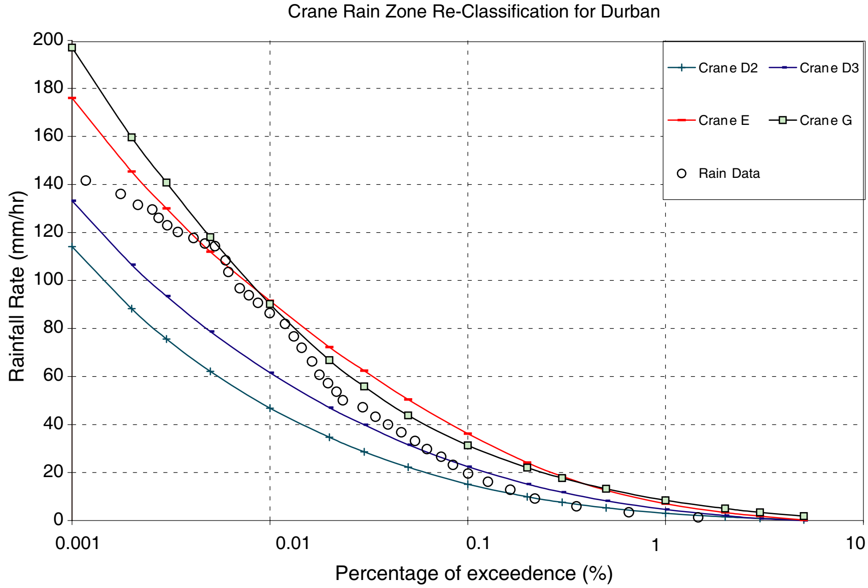

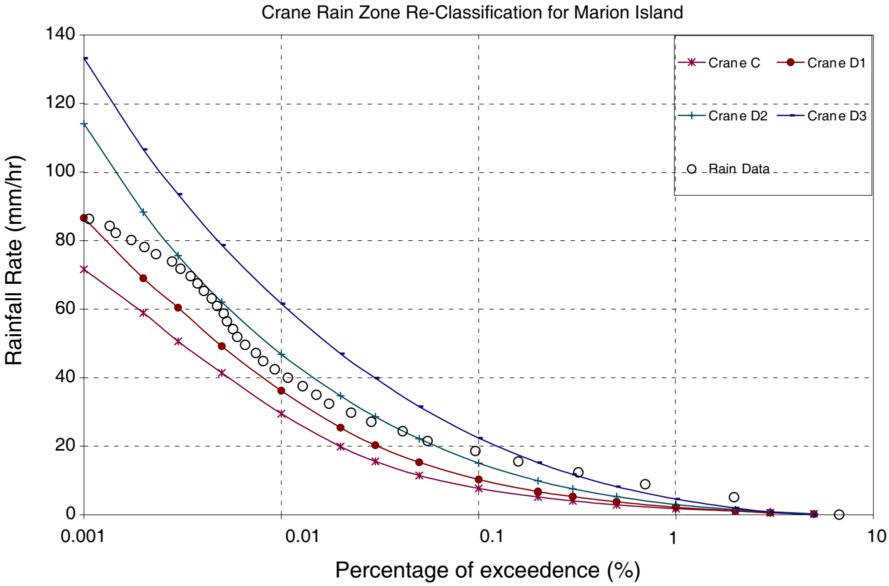

Figure 6. Crane rain classification re-zoning for South Africa and surrounding islands.

Table 6. Characteristic of rainfall rate climatic zone designation for both ITU-R and crane's models at 0.01%.

Location	ITU-R 1	ITU-R 5	Suggested ITU-R Designation	C-R Designation	Suggested C-R Designation
Port-Alfred	D-19	35	L-60	C-29.5	D_2-46.8
Bisho	D-19	35	L-60	D_1-36.2	D_2-46.8
Fort Beaufort	F-28	30	L-60	C-29.5	D_2-46.8
Umtata	F-28	30	L-60	D_1-36.2	D_3-61.6
Pretoria	E-22	55	L-60	D_2-46.8	D_2-46.8
Bethlehem	D-19	35	L-60	C-29.5	D_3-61.6
Durban	E-22	50	L-60	D_2-46.8	D_3-61.6
Spring	E-22	55	L-60	D_1-36.2	D_3-61.6
Ladysmith	E-22	50	L-60	D_2-46.8	D_3-61.6
Pietermaritzburg	E-22	45	L-60	D_2-46.8	D_3-61.6
Tshipise	F-28	50	K-42	D_1-36.2	D_1-36.2
Ermelo	E-22	50	L-60	F-22.2	D_3-61.6
Cape Town	D-19	35	E-22	C-29.5	C-29.5
Beaufort	D-19	25	F-28	C-29.5	C-29.5
Cape Point	D-19	25	K-35	C-29.5	D_1-36.2
Rustenburg	E-22	60	M-63	D_1-36.2	D_2-46.8
Klerksdorp	E-22	60	K-42	D_1-36.2	D_1-36.2
Kimberley	E-22	45	K-42	D_1-36.2	D_2-46.8
Upinton	E-22	35	K-42	D_1-36.2	D_1-36.2
Gough Island	D-19	40	K-42	C-29.5	D_1-36.2
Marion Island	A-8	40	K-42	A-9.9	D_1-36.2

where the ITU-R was over-estimated by 8.60% and 3.40% respectively. The results of these comparisons are shown in Table 4.

Table 4 consists of six columns: location, ITU-R 1 and ITU-R 5 with their respective rainfall rate values at 0.01% of exceedence. Other columns show suggested designations and remarks summing up the findings for both, the ITU-R and suggested designations. The table shows the newly enforced ITU-R P.837-5 has drastically improved the classification of rain climatic zone. This is supported by the research done in Singapore where the percentage difference reduces from 24% to 8% using ITU-R P.837-4 [17]. In this study, a difference as low as 2.44% from ITU-R P.837-5 and the newly assigned designation is observed. These are noted in stations such as Rustenburg and Marion

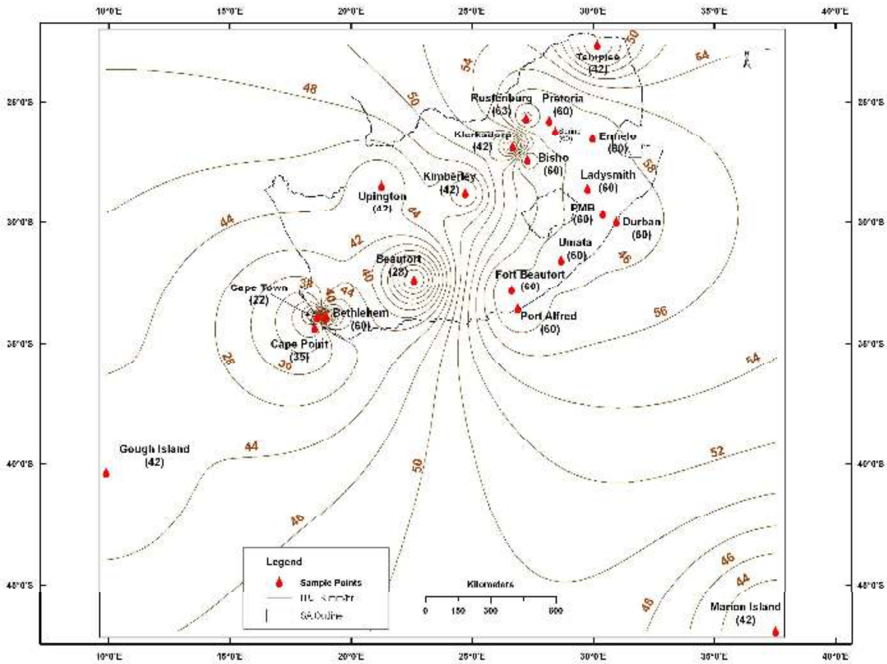

Figure 7. Contour plot using ITU-R designation at 0.01% for South Africa and surrounding islands.

Island. 4.34% differences are observed in Pretoria and springs. A worse situation of high percentage differences is observed in Fort Beaufort with a value of 33.33%. Comparing the new designation with ITU-R P837-1, it is observed that there is a wide difference, from a high 68% for Marion Island to the low of 7.32% for Cape Town. In Crane's rain climatic zones, the percentage difference is as low as 0% for Pretoria, and Beaufort, and as high as 57.04% in the case of Marion Island. In general, most sites showed that ITU-R P.837-5 under-estimate the rainfall rate value at 0.01% except in a few locations such as Cape Town and Klerksdorp. The Crane rain zones show under-estimation for all the sites except in cases where the old designation is the same as the proposed designations.

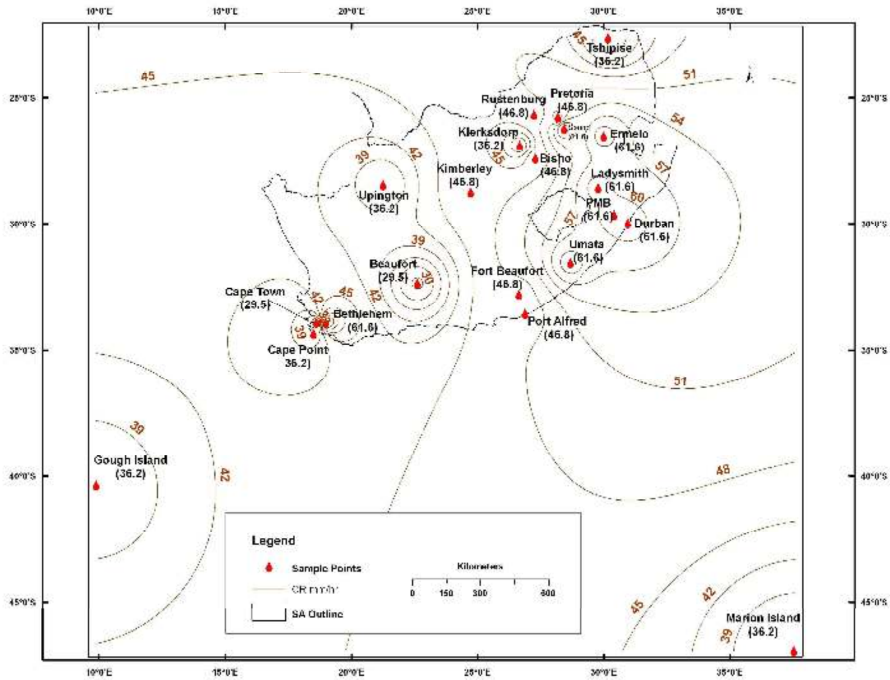

Figure 8. Contour plot using Crane designation at 0.01% for South Africa and surrounding islands.

6. RAINFALL RATE CONTOUR MAPS AT 0.01% OF PROBABILITY OF EXCEEDENCE

One common set back to empirical model and other models is lack the of enough network stations to adequately characterize a mapped region. This call for application of interpolation method in order to estimate the needed point based on the surrounded available data points. As recommended by ITU-R, bi-linear interpolation is considered as the most appropriate method for plotting contour maps. In this study, a simple inverse distance weighting (IDW) is used because of its inherent advantages such as the ability to consistently select grids point and effectively handle a disperse network of stations. These advantages are not too common with bi-linear interpolation. Another limitation to bi-linear interpolation is that the interpolation points are selected based on the numerical grid size, rather than the influence of physical distance. The IDW model uses the contributions of observed data points, summarizing their characteristics in the form of weighting to estimate the unknown points. The IDW expression is given by:

$$Z_j = K_j \sum_{i=1}^{n} \frac{1}{d_{ij}^{\alpha}} Z_i \tag{17}$$

where $K_j = \sum_{i=1}^{n} \frac{1}{d_{ij}}$ is the adjustment that optimizes the weighting to add up to 1 when the parameter $\alpha = 1$. Using this estimator, we are able to provide for the unknown data points and draw contour maps using both ITU-R predicted rain rate (RR) and Crane designation at 0.01% point for an easy application for radio planning engineers.

Figures 7 and 8 show the proposed rain climatic zones using a new proposed regional ITU-R and Crane model at 0.01% respectively. It is noted from both figures that the eastern part of the map experiences a higher rainfall rate distribution than the western part, with the exception of Bethlehem. This is as a result of the eastern wind from the Indian Ocean that hits the great escarpment that extends down to the tip of Bethlehem. Figures 7 and 8 confirmed the effect of the extensive wall, causing an orographic type of rainfall. In Figure 7, the tip of Cape Town, Upington and the islands recorded the lowest rainfall rate while the highest rainfall rate was recorded in the areas surrounded by the extensive coastal environment.

7. CONCLUSION

In this study, it is observed that the Western Cape region gets most of its rainfall in winter, while the rest of the country is generally a summer rainfall region. The additional factors that contribute to this variation are the striking contrast between temperatures on the country's east and west coasts, and the contribution of the warm Agulhas and cold Benguela currents that sweep the coastlines. Being in the Southern hemisphere, the seasons stand in opposition to those of Europe and North America.

The most widely used probability distributions were investigated using the maximum likelihood estimator to optimize the distributions. It was found that most of the studied areas were best defined by the Gamma distribution model, followed by Weibull distributions model, while Lognomal did well in very few sites. For the 21 stations, the Gamma model had an average χ^2 statistic of 10.8, followed by the Weibull model with an average of 19.85. The rest of the models gave an average χ^2 statistic of above 55, which is too close to the threshold 63.7 for 40 degree of freedom. The average root mean square percentage also gives evidence to the fact that the Gamma model is the most appropriate to describe most sites in South Africa and its surrounding islands.

It is found in some sites that the ITU-R model that was used over-estimates, while in many others sites the ITU-R model under-estimates, rainfall rate at defined points of probability of exceedences. Crane rain climatic zone designations had some exact matches in some sites as noted in Pretoria, Tshipise, Cape Town, Beaufort, Klerksdorp and Upington.

Rain contour maps have been identified as desirable tools for providing system designers, site engineers and network planners with estimated fade margins due to rain attenuation. The two plotted contour maps were optimized using statistical tool to satisfy accepted rainfall climatic zones defined by the ITU-R and Crane maps which are available in most radio planning tools. In this research, the contour map was developed using advanced Geographic Information Systems (GIS) tools with the adoption of IDW estimator to provide the contour map for rainfall rate at 0.01% of exceedence.

REFERENCES

1. Collin, R. E., *Antennas and Radiowave Propagation*, 401–402, McGraw Hill, ISBN 0-07-Y66156-1, 1995.
2. Goldhirsh, J., "Yearly variations of rain-rate statistics at wallops island and their impact on modeled slant path attenuation distributions," *IEEE Transaction on Antennas and Propagation*, Vol. 31, No. 6, 918–921, November 1983.
3. Crane, R. K., *Electromagnetic Wave Propagation Through Rain*, Wiley Interscience, New York, 1996.
4. ITU-R: Characteristics of Precipitation for Propagation Modeling, Recommendation P.837-4. ITU-R Recommendations, P Series, International Telecommunications Union, Geneva, 2007.
5. Rice, P. and N. Holmberg, "Cumulative time statistics of surface-point rainfall rate," *IEEE Transactions on Communications*, Vol. 21, 1772–1774, October 1973.
6. Moupfounma, F. and L. Martin, "Modelling of the rainfall rate cumulative distribution for the design of satellite and terrestrial communication systems," *International Journal of Satellite Communications*, Vol. 13, No. 2, 105–115, 1995.
7. Ajayi, G. O. and E. B. C. Ofoche, "Some tropical rainfall rate characteristics at ile-ife for microwave and millimeter wave application," *Journal of Climate and Applied Meteorology,* Vol. 23, 562–567, 1983.

8. Owolawi, P. A., T. J. Afullo, and S. B. Malinga, "Effect of rainfall on millimeter wavelength radio in Gough and Marion Islands," *PIERS Online*, Vol. 5, No. 4, 328–335, 2009.
9. Owolawi, P. A., T. J. Afullo, and S. B. Malinga, "Rainfall rate characteristics for the design of terrestrial links in South Africa," *Proceedings of Southern Africa Telecommunication Networks and Applications Conference (SATNAC)*, 1–76, September 2008.
10. Fashuyi, M. O., P. A. Owolawi, and T. J. Afullo, "Rainfall rate modeling for LOS radio systems in South Africa," *South African Institute of Electrical Engineering Journal*, Vol. 97, No. 1, 74–81, March 2006.
11. Owolawi, P. A. and T. J. Afullo, "Rainfall rate modeling and its worst month statistics for millimetric LOS links in South Africa," *Radio Science*, Vol. 42, 2007.
12. Owolawi, P. A., T. J. Afullo, and S. B. Malinga, "Effect of worst-month distribution on radio link design in South Africa," *11th URSI Commission F Triennial Open Symposium on Radio Wave Propagation and Remote Sensing*, 55–61, Rio de Janeiro, October 2007.
13. Mulangu, C. T., P. A. Owolawi, and T. J. O. Afullo, "Rainfall rate distribution for LOS radio system in Botswana," *Proceedings of 10th Southern Africa Telecommunication, Networks and Application Conference (SATNAC)*, Mauritius, September 2007.
14. Owolawi, P. A., "Rain rate and rain drop size distribution models for line-of-sight millimetric systems in South Africa," M.Sc. Dissertation, Department of Electrical and Electronics Engineering, University of KwaZulu Natal, Durban, 2006.
15. Seeber, R. J., "N model vir die bepaling van die punt-reenintensitverdeling vir die voorspelling van mikrogolf-reenverswakking in Suidelike Afrika," *South African Institute of Electrical Engineering Journal*, 67–75, June 1995.
16. Owolawi, P. A., "Characteristics of rain at microwave and millimetric bands for terrestrial and satellite links attenuation in south africa and surrounding islands," Ph.D. Dissertation, School of Electrical, Electronics and Computer Engineering, University of KwaZulu Natal, Durban, South Africa, 2010.
17. Emiliani, L. D., J. Agudelo, E. Gutierrez, J. Restrepo, and C. Fradique-Mendez, "Development of rain-attenuation and rain-rate maps for satellite system design in the Ku and Ka bands in Colombia," *IEEE Antennas and Propagation Magazine*, Vol. 46, No. 6, 54–68, December 2004.
18. *World Meteorological Organization: World Distribution of*

Thunderstorm Days, No. 21, TP. 21, WMO/OMM, Geneva, 1953.
19. *World Meteorological Organization: World Meteorological Organization Climatological Normal (CLINO) for Climate and Climate Ship Stations for the Period 1931–1960*, WMO/OMM, No. 117, TP. 52, Geneva, 1962.
20. Dutton, E. J., H. T. Dougherty, and R. F. Martin, Jr., "Prediction of European rainfall and link performance coefficients at 8 to 30 GHz," NTIS Rep., ACC-ACO-16-17, 1974.
21. Wong, R. K. W., "Weibull distribution, iterative likelihood techniques and hydrometeorlogical data," *Journal of Applied Meteorology*, Vol. 16, 1360–1364, 1977.
22. Wilks, D. S., "Rainfall intensity, the Weibull distribution and estimation of daily surface runoff," *Journal of Applied Meteorology*, Vol. 28, 52–58, 1989.
23. Evans, M., N. Hastings, and B. Peacock, *Statistical Distributions*, 2nd edition, John Wiley and Sons Inc., New York, 1993.
24. Walack, C., *Hand-book on Statistical Distributions for Experimentalists*, Internal Report SUF-PFY/96-01, University of Stockholm, 2007.
25. Eckhard, L., A. S. Werner, and A. Markus, "Lognormal distributions across the sciences: Key and clues," *BioScience*, Vol. 51, No. 5, May 2001.
26. Suhaila, J. and A. A. Jemain, "Fitting daily rainfall amount in Malaysia using the normal transformer distribution," *Journal of Applied Science*, Vol. 7, No. 14, 2007.
27. Thom, H. C., "A note on the gamma distribution," *Monthly Weather Review*, Vol. 86, 117–122, 1958.